Advanced Synthesis & Catalysis

DOI: 10.1002/adsc.201400125

Bipyridine Periodic Mesoporous Organosilica: A Solid Ligand for the Iridium-Catalyzed Borylation of C–H Bonds

Wolfram R. Grüning,[a] Georges Siddiqi,[a] Olga V. Safonova,[b] and Christophe Copéret[a,*]

[a] Department of Chemistry and Applied Biosciences, ETH Zurich, Vladimir-Prelog-Weg 2, 8093 Zurich, Switzerland
Fax: (+41)-44-633-1325; phone: (+41)-44-633-9394; e-mail: ccoperet@ethz.ch
[b] Paul Scherrer Institute, 5232 Villigen, Switzerland

Received: February 3, 2014; Published online: February 20, 2014

Supporting information for this article is available on the WWW under http://dx.doi.org/10.1002/adsc.201400125.

Abstract: With the goal to obtain a molecularly defined iridium(I) heterogeneous C–H functionalization catalyst, a *periodic mesoporous organosilica* (PMO) containing bipyridylene moieties in a matrix of biphenylene units as ligand platform was designed and fully characterized. The material exhibits a high surface area with small mesopores in a vermicular arrangement, and the pore walls show a highly crystal-like character. After surface passivation with chlorotrimethylsilane and functionalization with chloro(1,5-cyclooctadiene)iridium(I) dimer [{IrCl(COD)}$_2$] a molecularly defined Ir(I) surface complex was obtained according to EXAFS and UV-Vis spectroscopy. This functionalized material catalyzes the direct C–H borylation of arenes to yield the corresponding boronic esters and can be reused without significant loss of activity.

Keywords: C–H activation; heterogenous catalysis; iridium; organic-inorganic hybrid materials; periodic mesoporous organosilicas; surface chemistry

Combining the advantages of homogeneous and heterogeneous catalysts has been a major research effort in the past forty years, necessitating the elaboration of heterogeneous catalysts with definition on the molecular level.[1] One successful approach, called surface organometallic chemistry, has consisted in the controlled grafting of transition metal complexes directly on the surface of oxide materials.[2] In many instances, this approach has led to catalysts with performances close to or sometimes surpassing those of their homogeneous analogues. An alternative approach is the development of supported homogeneous catalysts, in which the metal center is coordinated to an organic ligand bound to high surface area materials.[3] Post-synthetic grafting of organic ligands on the oxide support has often led to deceiving results.[4] However major improvements have been achieved through the controlled incorporation of ligands in SBA-type materials by co-condensation of functional organotrialkoxysilanes and tetraethoxysilane in the presence of structure directing agents, giving rise to a more regular distribution of ligands within the pores of the material.[5] These materials enabled the generation of highly efficient and supported well-defined metal-based catalysts.[6] Towards the manufacture of heterogeneous catalysts with molecular precision, a promising class of materials has recently appeared: periodic mesoporous organosilicas (PMO).[7] Robust siloxane bridges hold together the organic linkers that constitute both the surface and the bulk of the material. PMOs are advantageous as they are highly ordered on the nanoscale: possessing small mesopores typically in a 2D hexagonal framework and exhibiting in many instances crystal-like ordering in the pore walls, especially when the organic linkers are arenes.[8] They thus provide a well-defined immediate environment making them ideal candidates as catalyst supports. Most PMOs prepared for catalytic applications so far rely on monodentate ligands[7e,9] with a few examples describing more elaborate systems such as phenylpyridine[10] or BINAP.[11,12]

In homogeneous catalysis, the Ir(I)-catalyzed direct borylation of C–H bonds[13] has been recognized as a mild and versatile reaction generating high value building blocks[14] directly from easily available starting materials.[15] To increase lifetime, ease product separation and avoid product contamination with metal traces, immobilization strategies such as a phosphine ligand bound to a silica surface have been proposed, however this system is limited to the directed activation of C–H bonds.[16] A second approach uses poorly soluble carboxylic acid bipyridine derivatives[17].

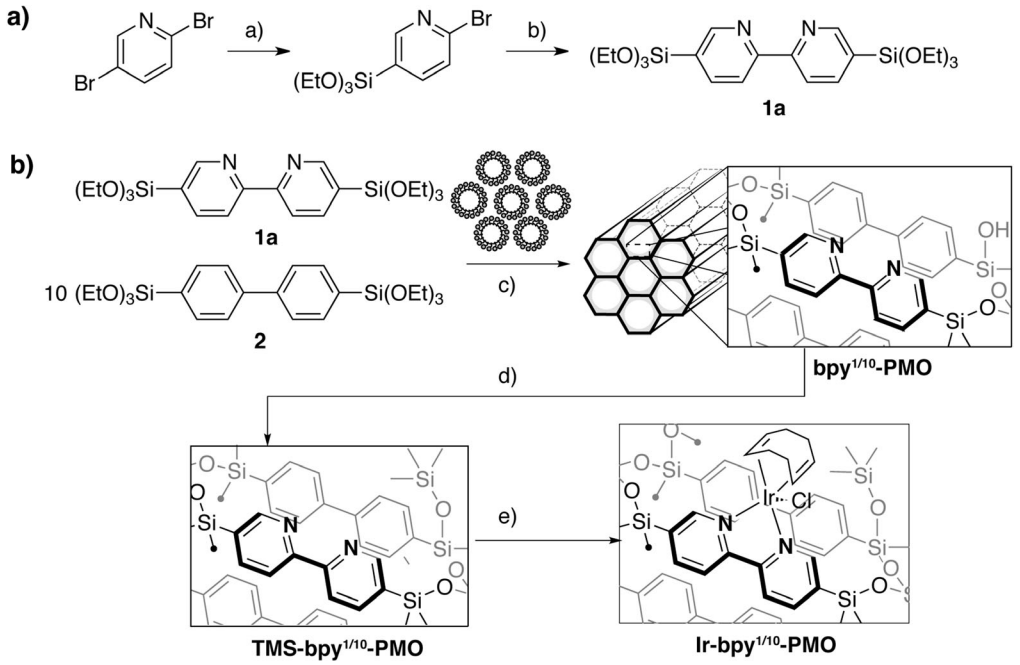

Scheme 1. a) Synthesis of precursor **1a** a) 1) *n*-BuLi, Et_2O, −95 °C, 1 h, 2) $MgCl_2$, −95 °C, 0.5 h, 3) $ClSi(OEt)_3$, −95 °C to 25 °C, 16 h, 40%; b) $Ni(PPh_3)_2Br_2$, Zn*, NBu_4I, THF, 70 °C, 16 h, 53%. **b)** Synthesis of materials c) n-$C_{18}H_{37}NMe_3$, H_2O, NaOH, 25 °C, 24 h, 97 °C, 21 h; d) TMSCl, $NEt(i\text{-}Pr)_2$, THF, 25 °C, 16 h; e) $[\{IrCl(COD)\}_2]$, CH_2Cl_2, 30 min.

Since one of the most promising homogeneous catalysts for C–H borylation is based on $[\{IrX(COD)\}_2]$ (X = OMe, Cl) activated by bipyridine ligands, we have developed a heterogeneous catalyst based on the coordination of an Ir(I) molecular precursor to bipyridine moieties in the walls of a PMO. Towards this goal a PMO containing bipyridylene units site dispersed in a biphenylene matrix, for improved site isolation,[18] was prepared and successfully functionalized by $[\{IrCl(COD)\}_2]$.

In order to prepare the bipyridine-containing PMO, 5,5′-bis(triethoxysilyl)-2,2′-bipyridine (**1a**) was synthetized in two steps *via* a regioselective lithiation of 2,5-dibromopyridine followed by a nickel(II)-catalyzed reductive coupling (Scheme 1, a). The material **bpy$^{1/10}$-PMO** was then synthesized by the hydrolysis and co-condensation of **1a** (1 equiv.) and 4,4′-bis(triethoxysilyl)-1,1′-biphenyl **2** (10 equiv.) in dilute aqueous sodium hydroxide solution in the presence of trimethylstearylammonium chloride as structure directing agent (SDA) as outlined in Scheme 1, b.

The parent material **bpy$^{1/10}$-PMO** exhibits good structuration as shown in Figure 1. Nitrogen adsorption and desorption experiments give rise to a type IV isotherm with a small hysteresis loop (Figure 1, a) typical for materials with small mesopores.[18,19] Analysis according to the Brunau–Emmett–Teller model[20] yields a surface area of 690 $m^2 g^{-1}$, and the maximum of the pore-size distribution was calculated to be *ca.* 2.4 nm at the limit of Barrett–Joyner–Halenda[21] analysis. Small angle X-ray diffraction (see the Supporting Information) gives rise to a single broad peak at 1.9° corresponding to a lattice constant of 4.7 nm indicating a vermicular rather than a perfectly 2D hexagonal structure. The combined values for pore size and periodicity give a pore wall thickness of *ca.* 2 nm; a relatively large value, as PMOs of this type typically give rise to walls of a few molecular layers.[8,10] In the pore walls the material shows a high degree of ordering as evident by powder X-ray diffraction (Figure 1, b). Five sharp peaks are observed at $2\Theta/° = 7.5$, 15, 23, 31, 38, they can be assigned to a periodic structure of 1.16 nm and the corresponding higher order reflections. This value is in good agreement with the length of the biaryl fragments and values for similar materials reported earlier.[8b,10a] Transmission electron microscopy (Figure 1 c, d) confirms the presence of a porous structure and also shows molecular scale periodicity perpendicular to the pore direction. The structural features are homogenously distributed throughout the material (see the Supporting Information).

The infrared spectrum of the material (see the Supporting Information, Figures S3–S5) shows a sharp band at 3720 cm^{-1} characteristic of isolated silanol groups, as well as aromatic C–H bands at 3070 and 3024 cm^{-1}. Furthermore the characteristic vibrations of the aromatic rings are observed at 1604 cm^{-1} with a shoulder at 1580 cm^{-1} corresponding to the most intense ring deformation bands of **2** (1600 cm^{-1}) and **1a** (1580 cm^{-1}), respectively.

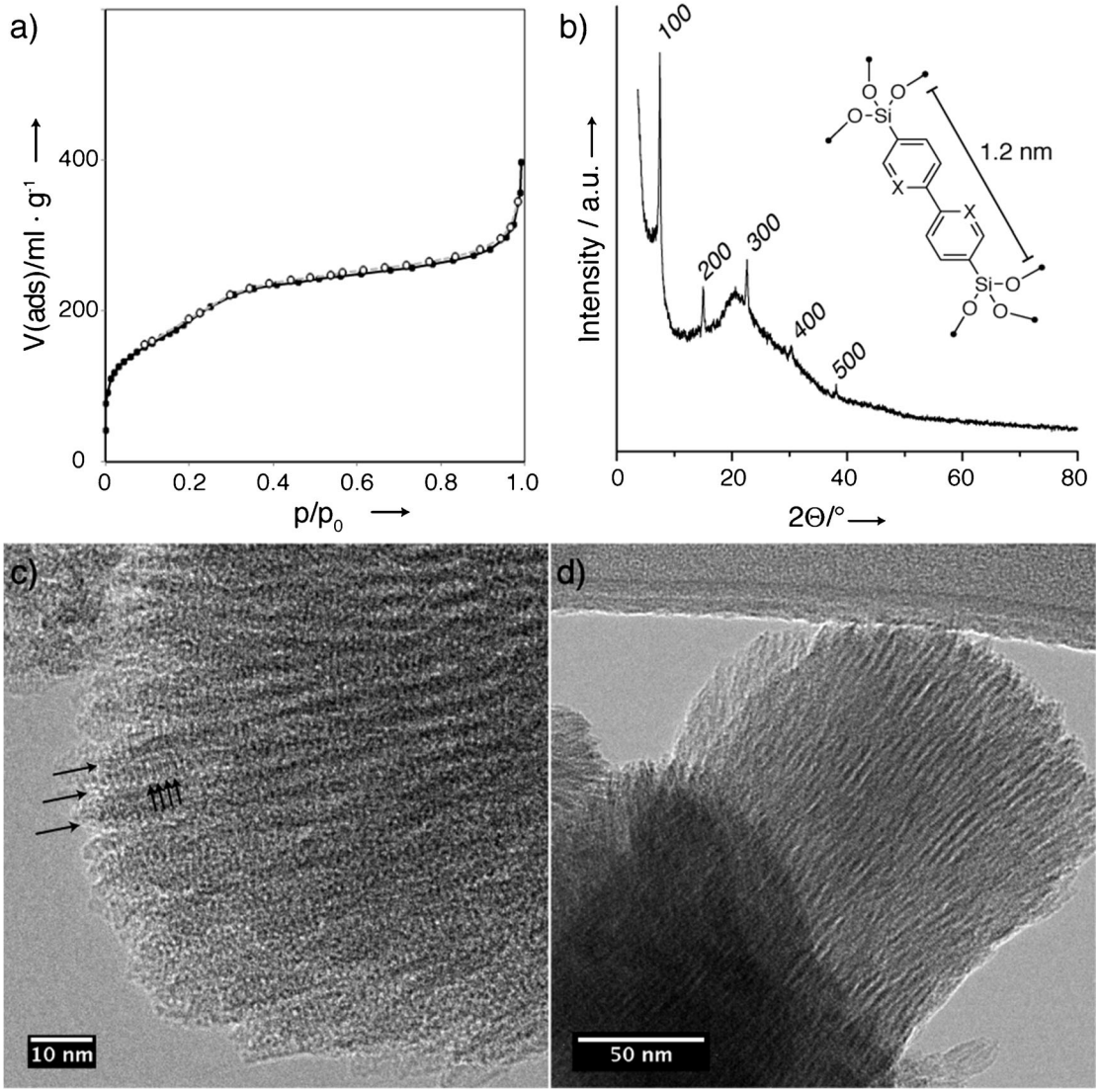

Figure 1. Textural properties of **bpy$^{1/10}$-PMO**: a) nitrogen adsorption/desorption isotherm at 77 K; b) p-XRD pattern showing reflections corresponding to a distance of 1.2 nm; c) high magnification showing TEM showing molecular scale and pore structure periodicity; d) lower magnification image showing the porous structure.

Bpy$^{1/10}$-PMO was also characterized by solid state NMR spectroscopy; the obtained spectra are shown in Figures S1 and S2 (Supporting Information). The ^{13}C-cross-polarization magic angle spinning (CP-MAS) NMR spectrum of the parent material **bpy$^{1/10}$-PMO** in Figure S1 (Supporting Information) is dominated by the four resonances of the biphenylene groups at 142, 135, 131, and 126 ppm.[8b] A fifth lower intensity resonance, well separated, at 155 ppm is observed and is characteristic for the α-carbons in the bipyridine. The remaining resonances of the bipyridylene fragment are buried under the biphenylene component.

The ^{29}Si CP-MAS spectrum (Figure S2, Supporting Information) shows exclusively T-sites, the major peak is observed at −77 ppm and corresponds to the T^3-sites of the biphenylene units and bipyridylene units. A second peak at −70 ppm corresponds to incompletely condensed T^2 sites, probably residing at the surface of the material. No Q-sites are observed emphasizing the stability of the C–Si bond.

The surface of the material was passivated with chlorotrimethylsilane (Scheme 1, b) to give **TMS-bpy$^{1/10}$-PMO**, prior to coordination of the Ir(I) molecular precursor on the bipyridylene moieties to minimize unwanted surface interactions. The IR spectrum (Figures S3 and S4, Supporting Information) shows the disappearance of the isolated silanol band at 3720 cm^{-1} and the appearance of alkyl C–H bands at 2975 cm^{-1}. NMR spectroscopy also shows the appearance of characteristic TMS resonances at −2 ppm in the ^{13}C spectrum (Figure S1, Supporting Information)

and at 14 ppm in the ^{29}Si spectrum (Figure S2, Supporting Information). **TMS-bpy$^{1/10}$-PMO** was then reacted with chloro(1,5-cyclooctadiene)iridium(I) dimer [{IrCl(COD)}$_2$] to give a light blue green material **Ir-bpy$^{1/10}$-PMO**. The iridium content of the material was found to be 1.5% by elemental analysis, which corresponds to a functionalization of *ca.* 30% of the bipyridylene units in the framework of the material. It is noteworthy that dark-field transmission electron microscopy (Supporting Information) shows isolated iridium centers spread over the whole material. The absence of Ir rich patches is thus consistent with a good distribution of the bipyridylene units within the material matrix. The ^{29}Si NMR spectrum (Figure S2, Supporting Information) remains unchanged, showing that complexation does not lead to any modification of the structure of the material. In addition, all textural properties such as surface area and pore size of **bpy$^{1/10}$-PMO** are well preserved in the materials **TMS-bpy$^{1/10}$-PMO** and **Ir-bpy$^{1/10}$-PMO** (Supporting Information).

No major changes are observed in the ^{13}C NMR spectra of **Ir-bpy$^{1/10}$-PMO**, mainly because of the high dilution of functionalized species. The surface functionalization in **Ir-bpy$^{1/10}$-PMO** was also monitored by UV-Vis spectroscopy (Figure 2 and Supporting Information, Figure S12). The parent material shows a flat base line up to 320 nm before saturation. The functionalized material however shows a distinct band at 620 nm that is in good agreement with the analogous homogeneous complex **3** showing an absorption maximum at 600 nm (the preparation and structural characterization of **3** is given in the Supporting Information).

The structure of the surface complex was established by X-ray absorption near edge spectroscopy (XANES) and extended X-ray absorption fine-structure (EXAFS) at the Ir L_3 edge.[22] The XANES spectra for [{IrCl(COD)}$_2$] and **Ir-bpy$^{1/10}$-PMO** (Supporting Information, Figure S7) show nearly identical absorption edges, confirming the conservation of the oxidation state of Ir(I) upon complexation. Furthermore, EXAFS fitting (Table 1; Supporting Information, Figures S8 and S10) is consistent with iridium coordinated to a bipyridine unit by two nitrogen centers at 2.05 Å, to a COD ligand by four carbon centers at 2.10 Å, and a chlorine center at 2.34 Å in the first coordination shell. Excluding Cl from the first coordination sphere of Ir is detrimental to the fit quality (Figure S11, Supporting Information). Further improvement of the fit was achieved by inclusion of second neighbor shell consisting of four COD carbons and four bipyridine carbons (Figure S8, Supporting Information). These results confirm the formation of a molecularly defined, pentacoordinate [Ir(I)Cl(COD)**bpy^{PMO}**] surface complex. These complexes are homogenously distributed within the materials (Supporting Information).

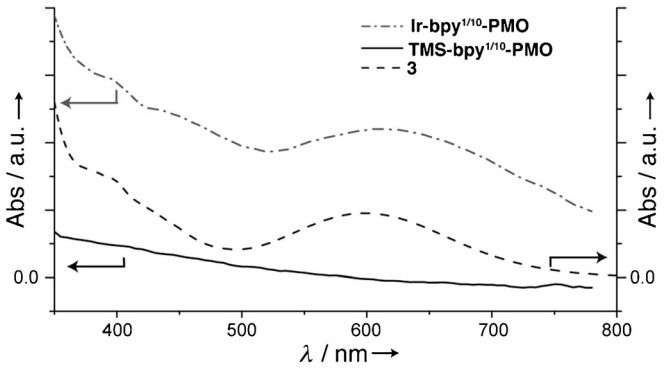

Figure 2. UV-Vis spectra; left axis absorbance of materials based on diffuse reflectance spectra and conversion with Abs = log(R^{-1}). Right axis absorbance of **3** (1.8 mM/CH_2Cl_2).

Table 1. Illustration of the surface complex in **Ir-bpy$^{1/10}$-PMO** and summary of EXAFS analysis: *N* is the number of centers, R is the interatomic distance, σ^2 is the Debye-Waller factor, E_0 is the energy shift. The passive electron reduction factor $SO_2 = 0.86$ was fixed to the value obtained for [{IrCl(COD)}$_2$].

	Center	Fragment	*N*	R [Å]	σ^2 [Å^2]	E_0 [eV]
1st shell	N	1-bpy	2	2.05(1)	0.0047(6)	5.7(6)
	C	α-COD	4	2.10(1)	0.0047(6)	5.7(6)
	Cl	–	1	2.34(1)	0.0047(6)	5.7(6)
2nd shell	C	2-bpy	2	2.61(4)	0.010(5)	5.7(6)
	C	β-COD	4	2.98(3)	0.010(5)	5.7 (6)
	C	6-bpy	2	2.77(4)	0.010(5)	5.7 (6)

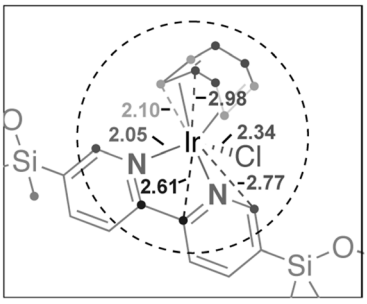

We then examined the catalytic performance of **Ir-bpy$^{1/10}$-PMO** for the C–H bond functionalization of a series of arenes with bis(pinacolato)diboron (B_2pin_2) as shown in Table 2. In the presence of 0.8 mol% of Ir, B_2pin_2 reacts quantitatively with benzene in 24 h to give exclusively PhBpin, similarly to the corresponding homogeneous catalysts.[13b] No reaction (<1%) was observed in the absence of Ir or **bpy$^{1/10}$-PMO** (Table 2, entries 2 and 3). We attribute the catalytic activity to the presence of both the bipyridine containing material and the iridium surface functionalization. It is also noteworthy that following an induction period the reaction is pseudo 0 order in

Table 2. Catalytic tests for C–H activation and borylation.

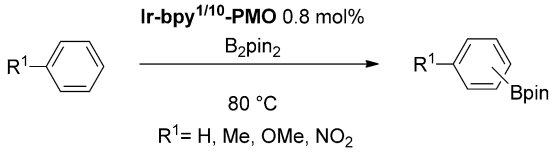

Entry	Catalyst	Arene	Time [h]	Conversion[a]	Yield[b]
1	**Ir-bpy$^{1/10}$-PMO**	benzene	24	95%[c]	76%[c]
2	**bpy$^{1/10}$-PMO**	benzene	24	0%	–
3	[{IrCl(COD)}$_2$][d]	benzene	24	<1%	–
4	[{IrCl(COD)}$_2$]/bpy[e]	benzene	16	n.r.[f]	95%
5	**Ir-bpy$^{1/10}$-PMO**	benzene-d_6	21	>99%	78%
6	**Ir-bpy$^{1/10}$-PMO**	toluene	24	99%	87%
7	**Ir-bpy$^{1/10}$-PMO**	anisole	24	90%	64%
8	**Ir-bpy$^{1/10}$-PMO**	nitrobenzene	24	40%	10%

[a] Conversion of B_2pin_2 based on GC.
[b] GC yield based on hexamethylbenzene as internal standard.
[c] Corresponds to a TOF = 5 h^{-1} and 4 h^{-1}.
[d] 8 mol% catalyst loading was used.
[e] 3 mol%, taken from ref.[13b]
[f] Not reported.

benzene, due to its large excess. Under these conditions, the turnover frequency (TOF) reaches 4 h^{-1}, which is similar to or somewhat higher than that of the originally reported homogeneous system (TOF = 2 h^{-1}).[13b] **Ir-bpy$^{1/10}$-PMO** also shows good conversion with substituted and electron-rich arenes (Table 2, entries 6 and 7), both toluene and anisole lead to almost full conversion (>90%) of B_2pin_2 after 24 h. However, the very electron-poor nitrobenzene (Table 2, entry 8) gave only a conversion of 40% under identical conditions, probably due to deactivation of the catalyst.

For mono-substituted arenes, the regioselectivity is close to what is expected from a statistical activation of the C–H bond of the *meta*- and *para*-positions of the arenes. The selectivity patterns (%: *o*/*m*/*p*) observed are very similar for toluene (0/64/36), anisole (0/71/29), and nitrobenzene (0/71/29) as it was also observed in the homogeneous systems (0/69/31) and (1/74/25) for toluene and anisole, respectively.[13b] The similar activity and regioselectivity of the molecular and the surface complexes indicate the molecular nature of the active sites in these materials. The stability of the catalytic system was evaluated, the catalyst (0.8 mol%) was used in three consecutive runs with the same loadings of reactants, which led each time to greater than 90% conversion with no apparent loss of activity for both toluene or anisole. In fact, the reaction profile (0 order in benzene with similar TOF) showed virtually identical behavior upon re-addition of diborane (Supporting Information). Furthermore, the catalyst loading in the case of benzene could be reduced to 0.1 mol% yielding 64% conversion after 15 days corresponding to a turnover number of 640. Note however that the catalytic activity decreased non-linearly hinting towards the partial deactivation of the catalyst at this loading. The catalyst wash-off showed no significant iridium content ($\leq$ 1 ppm), except for nitrobenzene where about 5 ppm are detected, consistent with the much lower observed conversion and the fast deactivation of the catalyst.

In conclusion, the synthesis of a periodic mesoporous organosilica containing bipyridylene units in the pore walls and its subsequent functionalization was achieved to yield a molecularly-defined surface iridium complex. The synthesized materials display good catalytic performances for the C–H bond functionalization of arenes to arylboronic esters, in close resemblance to the homogenous catalyst based on [{IrCl(COD)}$_2$] and 4,4′-bis-*tert*-butyl-2,2-bipyridine. These materials open new avenues in the development of well-defined heterogeneous catalysts, and we are currently exploring methods to enhance their activity and stability through rational design.

Experimental Section

Full experimental details can be found in the Supporting Information.

Synthesis of bpy$^{1/10}$-PMO

In a 100-mL PTFE cylinder trimethylstearylammonium chloride (0.715 g, 2.05 mmol) was dissolved in water (44.2 mL) and NaOH (6 M, 0.74 mL, 4.4 mmol) was added. The solution was stirred for 1 hour and then a mixture of **1** (275 mg, 0.57 mmol, 1.0 equiv.) and 4,4′-bis(triethoxysilyl)-1,1′-biphenyl **2** (2.72 g, 57.0 mmol, 10 equiv.) was added

dropwise. The solution was stirred at 25 °C for 24 h and then heated to 97 °C without stirring for 24 h. The resulting white powder was filtered off and washed with water (120 mL × 3), acetone (120 mL × 5), and Et_2O (120 mL). The material was dried under vacuum (10^{-5} mbar) at 85 °C. The material was then suspended in ethanol (200 mL) and hydrochloric acid (2 M, 3.8 mL) and stirred for 16 h. The material was filtered off and washed with water (100 mL × 3), acetone (100 mL × 3), and Et_2O (20 mL × 3). After drying under vacuum (10^{-5} mbar) at 85 °C **bpy$^{1/10}$-PMO** was obtained as white powder; yield: 1.14 g.

Surface Passivation TMS-bpy$^{1/10}$-PMO

bpy$^{1/10}$-PMO (320 mg) was suspended in THF (5 mL) and NEt(*i*-Pr)$_2$ (0.42 mL, 2.4 mmol) and TMSCl (0.25 mL, 2.0 mmol) were added. The suspension was stirred for 16 h at 25 °C. Methanol (0.10 mL, 0.25 mmol) was added and stirring was continued before the suspension was filtered and the filter cake washed with THF/NEt(*i*-Pr)$_2$ 9:1 (5 mL × 2), THF (10 mL × 3), acetone (10 mL × 3), and Et_2O (10 mL × 3). The material was dried under vacuum (10^{-5} mbar) at 140 °C to give **TMS-bpy$^{1/10}$-PMO**; yield: 280 mg.

Synthesis of Ir-bpy$^{1/10}$-PMO

The material **TMS-bpy$^{1/10}$-PMO** (210 mg) was charged into a two-chambered Schlenk flask connected by a sintered glass frit. To the material a solution of [{IrCl(COD)}$_2$] (40 mg, 0.06 mmol) in CH_2Cl_2 (6 mL) was added to the material. The suspension was stirred for 30 min, filtered and then washed by 3 cycles of solvent vacuum transfer and filtration. The material was subsequently dried at 25 °C under high vacuum (10^{-5} mbar) to give **Ir-bpy$^{1/10}$-PMO**; yield: 170 mg. Care should be taken in handling this material as it is highly air-sensitive.

Catalytic Test: General Procedure

In a glovebox under an argon atmosphere a 2-mL HPLC vial was charged with **Ir-bpy$^{1/10}$-PMO** (10 mg, 0.8 μmol Ir, 0.8 mol%) and B_2pin_2 (24 mg, 0.10 mmol, 1.0 equiv.). The corresponding substrate (60 equiv.) was then added neat with a syringe. The resulting suspension was immersed into a sandbath heated to 80 °C and stirred for 24 h. Aliquots were taken, diluted in Et_2O and analyzed by GC (Agilent HP-1MS, He). The retention times were calibrated with known standards. The relative intensity was calibrated with hexamethylbenzene as internal standard.

Acknowledgements

We thank Dr. Alexey Fedorov for fruitful discussions and Dr. Maryna Bodnarchuk and Dr. Frank Krumeich for TEM micrographs.

References

[1] a) C. Copéret, M. Chabanas, R. Petroff Saint-Arroman, J.-M. Basset, *Angew. Chem.* **2003**, *115*, 164–191; *Angew. Chem. Int. Ed.* **2003**, *42*, 156–181; b) J. M. Thomas, R. Raja, D. W. Lewis, *Angew. Chem.* **2005**, *117*, 6614–6641; *Angew. Chem. Int. Ed.* **2005**, *44*, 6456–6482; c) M. Tada, Y. Iwasawa, *Coord. Chem. Rev.* **2007**, *251*, 2702–2716; d) M. Tada, K. Motokura, Y. Iwasawa, *Top. Catal.* **2008**, *48*, 32–40; e) S. L. Wegener, T. J. Marks, P. C. Stair, *Acc. Chem. Res.* **2012**, *45*, 206–214; f) H. Tüysüz, F. Schüth, in *Advances in Catalysis*, Vol. 55, (Eds.: C. G. Bruce, C. J. Friederike), Academic Press, New York, **2012**, pp 127–239.

[2] F. Rascon, R. Wischert, C. Copéret, *Chem. Sci.* **2011**, *2*, 1449–1456.

[3] a) A. Stein, B. J. Melde, R. C. Schroden, *Adv. Mater.* **2000**, *12*, 1403–1419; b) F. Hoffmann, M. Cornelius, J. Morell, M. Fröba, *Angew. Chem.* **2006**, *118*, 3290–3328; *Angew. Chem. Int. Ed.* **2006**, *45*, 3216–3251.

[4] a) C. Copéret, J. M. Basset, *Adv. Synth. Catal.* **2007**, *349*, 78–92; b) N. Gartmann, D. Brühwiler, *Angew. Chem.* **2009**, *121*, 6472–6475; *Angew. Chem. Int. Ed.* **2009**, *48*, 6354–6356.

[5] a) M. H. Lim, A. Stein, *Chem. Mater.* **1999**, *11*, 3285–3295; b) T. Yokoi, H. Yoshitake, T. Tatsumi, *J. Mater. Chem.* **2004**, *14*, 951–957; c) J. Nakazawa, T. D. P. Stack, *J. Am. Chem. Soc.* **2008**, *130*, 14360–14361; d) J. H. Ramm, N. Gartmann, D. Brühwiler, *J. Colloid Interface Sci.* **2010**, *345*, 200–205; e) M. Sharifi, R. Marschall, M. Wilhelm, D. Wallacher, M. Wark, *Langmuir* **2011**, *27*, 5516–5522; f) M. Wessig, M. Drescher, S. Polarz, *J. Phys. Chem. C.* **2013**, *117*, 2805–2816.

[6] a) T. J. Terry, T. D. P. Stack, *J. Am. Chem. Soc.* **2008**, *130*, 4945–4953; b) T. K. Maishal, J. Alauzun, J.-M. Basset, C. Copéret, R. J. P. Corriu, E. Jeanneau, A. Mehdi, C. Reyé, L. Veyre, C. Thieuleux, *Angew. Chem.* **2008**, *120*, 8782–8784; *Angew. Chem. Int. Ed.* **2008**, *47*, 8654–8656; c) I. Karamé, M. Boualleg, J.-M. Camus, T. K. Maishal, J. Alauzun, J.-M. Basset, C. Copéret, R. J. P. Corriu, E. Jeanneau, A. Mehdi, C. Reyé, L. Veyre, C. Thieuleux, *Chem. Eur. J.* **2009**, *15*, 11820–11823; d) J. Nakazawa, B. J. Smith, T. D. P. Stack, *J. Am. Chem. Soc.* **2012**, *134*, 2750–2759; e) M. K. Samantaray, J. Alauzun, D. Gajan, S. Kavitake, A. Mehdi, L. Veyre, M. Lelli, A. Lesage, L. Emsley, C. Copéret, C. Thieuleux, *J. Am. Chem. Soc.* **2013**, *135*, 3193–3199; for reviews see: f) S. Shylesh, M. Jia, W. R. Thiel, *Eur. J. Inorg. Chem.* **2010**, *2010*, 4395–4410; g) A. Zamboulis, N. Moitra, J. J. E. Moreau, X. Cattoen, M. Wong, C. Man, *J. Mater. Chem.* **2010**, *20*, 9322–9338; h) U. Diaz, D. Brunel, A. Corma, *Chem. Soc. Rev.* **2013**, *42*, 4083–4097.

[7] a) S. Inagaki, S. Guan, Y. Fukushima, T. Ohsuna, O. Terasaki, *J. Am. Chem. Soc.* **1999**, *121*, 9611–9614; b) T. Asefa, M. J. MacLachlan, N. Coombs, G. A. Ozin, *Nature* **1999**, *402*, 867–871; c) B. J. Melde, B. T. Holland, C. F. Blanford, A. Stein, *Chem. Mater.* **1999**, *11*, 3302–3308; d) K. J. Shea, J. Moreau, D. A. Loy, R. J. P. Corriu, B. Boury, in: *Functional Hybrid Materials*, Wiley-VCH, Weinheim, **2003**, pp 50–85; e) F. Hoffmann, M. Fröba, *Chem. Soc. Rev.* **2011**, *40*, 608–620; f) N. Mizoshita, T. Tani, S. Inagaki, *Chem. Soc. Rev.* **2011**, *40*, 789–800.

[8] a) S. Inagaki, S. Guan, T. Ohsuna, O. Terasaki, *Nature* **2002**, *416*, 304–307; b) M. P. Kapoor, Q. Yang, S. Inagaki, *J. Am. Chem. Soc.* **2002**, *124*, 15176–15177.
[9] a) A. Kuschel, M. Drescher, T. Kuschel, S. Polarz, *Chem. Mater.* **2010**, *22*, 1472–1482; b) M. Waki, N. Mizoshita, T. Ohsuna, T. Tani, S. Inagaki, *Chem. Commun.* **2010**, *46*, 8163–8165.
[10] a) M. Waki, N. Mizoshita, T. Tani, S. Inagaki, *Angew. Chem.* **2011**, *123*, 11871–11875; *Angew. Chem. Int. Ed.* **2011**, *50*, 11667–11671; b) W. R. Grüning, A. J. Rossini, A. Zagdoun, D. Gajan, A. Lesage, L. Emsley, C. Copéret, *Phys. Chem. Chem. Phys.* **2013**, *15*, 13270–13274.
[11] T. Seki, K. McEleney, C. M. Crudden, *Chem. Commun.* **2012**, *48*, 6369–6371.
[12] 2,2′-Bis(diphenylphosphino)-1,1′-binaphthyl.
[13] a) T. Ishiyama, J. Takagi, J. F. Hartwig, N. Miyaura, *Angew. Chem.* **2002**, *114*, 3182–3184; *Angew. Chem. Int. Ed.* **2002**, *41*, 3056–3058; b) T. Ishiyama, J. Takagi, K. Ishida, N. Miyaura, N. R. Anastasi, J. F. Hartwig, *J. Am. Chem. Soc.* **2002**, *124*, 390–391; c) J.-Y. Cho, M. K. Tse, D. Holmes, R. E. Maleczka, M. R. Smith, *Science* **2002**, *295*, 305–308.
[14] a) N. Miyaura, in: *Cross-Coupling Reactions*, Vol. 219, (Ed.: N. Miyaura), Springer, Berlin, Heidelberg, **2002**, pp 11–59; b) N. Miyaura, in: *Metal-Catalyzed Cross-Coupling Reactions*, Wiley-VCH, Weinheim, **2004**, pp 41–123; c) D. G. Hall, in: *Boronic Acids*, Wiley-VCH, Weinheim, **2005**, pp 1–99.
[15] a) I. A. I. Mkhalid, J. H. Barnard, T. B. Marder, J. M. Murphy, J. F. Hartwig, *Chem. Rev.* **2010**, *110*, 890–931; b) J. F. Hartwig, *Acc. Chem. Res.* **2012**, *45*, 864–873; c) J. F. Hartwig, *Chem. Soc. Rev.* **2011**, *40*, 1992–2002; d) S. M. Preshlock, B. Ghaffari, P. E. Maligres, S. W. Krska, R. E. Maleczka, M. R. Smith, *J. Am. Chem. Soc.* **2013**, *135*, 7572–7582.
[16] a) S. Kawamorita, H. Ohmiya, K. Hara, A. Fukuoka, M. Sawamura, *J. Am. Chem. Soc.* **2009**, *131*, 5058–5059; b) S. Kawamorita, R. Murakami, T. Iwai, M. Sawamura, *J. Am. Chem. Soc.* **2013**, *135*, 2947–2950.
[17] a) T. Tagata, M. Nishida, A. Nishida, *Tetrahedron Lett.* **2009**, *50*, 6176–6179; b) T. Tagata, M. Nishida, A. Nishida, *Adv. Synth. Catal.* **2010**, *352*, 1662–1666.
[18] S. Mascotto, D. Wallacher, A. Kuschel, S. Polarz, G. A. Zickler, A. Timmann, B. M. Smarsly, *Langmuir* **2010**, *26*, 6583–6592.
[19] a) M. Kruk, M. Jaroniec, *Chem. Mater.* **2001**, *13*, 3169–3183; b) K. S. W. Sing, F. Rouquerol, J. Rouquerol, P. Llewellyn, in: *Adsorption by Powders and Porous Solids*, 2nd edn., (Eds.: F. Rouquerol, J. Rouquerol, K. S. W. Sing, P. Llewellyn, G. Maurin), Academic Press, Oxford, **2014**, pp 269–302.
[20] S. Brunauer, P. H. Emmett, E. Teller, *J. Am. Chem. Soc.* **1938**, *60*, 309–319.
[21] E. P. Barrett, L. G. Joyner, P. P. Halenda, *J. Am. Chem. Soc.* **1951**, *73*, 373–380.
[22] S. Bordiga, E. Groppo, G. Agostini, J. A. van Bokhoven, C. Lamberti, *Chem. Rev.* **2013**, *113*, 1736–1850.

